

Effects of the exciton continuum on resonant Raman scattering in GaAs quantum wells

Guozhong Wen and Yia-Chung Chang

Department of Physics and Materials Research Laboratories, University of Illinois at Urbana-Champaign, Urbana, Illinois 61801

(Received 3 January 92)

The effect of the exciton continuum on resonant Raman scattering in GaAs quantum wells is investigated. A \mathbf{k} -space sampling technique is used to deal with exciton states, including the effects of valence-band mixing. Discrete and continuum exciton states are included in our calculation. We find that the resonant Raman spectra so obtained are in much better agreement with experiment compared with those that do not include the exciton continuum states.

Resonant Raman scattering (RRS) is very useful for studying the properties of exciton and phonon states as well as the electron-phonon interaction in quantum wells. Recently Zhu, Huang, and Tang¹ presented a microscopic theory for the resonant Raman spectrum mediated by exciton states in multiple quantum wells. In their calculation only discrete exciton states were considered. In this paper, we present our calculation of the RRS spectra of GaAs quantum wells, including the effects of exciton con-

tinuum states. This is accomplished with the use of the \mathbf{k} -space sampling technique recently developed by Chu and Chang.² We show that with the inclusion of exciton continuum states, the predicted theoretical spectra are in excellent agreement with data obtained by Zucker *et al.*³

Raman efficiency for $z\bar{z}$ backscattering is proportional to¹

$$|\hat{\epsilon}_s \cdot \vec{R} \cdot \hat{\epsilon}_i|^2 \sim \left| \frac{1}{m_0} \sum_{\alpha, \beta} \frac{\langle 0 | P \cdot \hat{\epsilon}_s | \beta \rangle \langle \beta | H_{e-ph} | \alpha \rangle \langle \alpha | P \cdot \hat{\epsilon}_i | 0 \rangle}{(E_\alpha - E)(E_\beta + \hbar\omega_s - E)} \right|^2, \tag{1}$$

where $\hat{\epsilon}_i$ and $\hat{\epsilon}_s$ are polarization vectors for incident and scattered light, respectively. $\hbar\omega_s$ is the s th LO-phonon energy. $|\alpha\rangle$ and $|\beta\rangle$ denote the intermediate exciton states associated with energies E_α and E_β . We adopt the expression for the Fröhlich interaction between an electron and an s th confined LO-phonon mode given by Zhu, Huang, and Tang,¹

$$H_{e-ph}(z) = iA_s \Phi_s(z) \tag{2}$$

$$= \begin{cases} iA_s \{ \cos [s\pi z / (p+1)a] - (-1)^{s/2} \} & \text{for } s=\text{even} \\ iA_s \{ \sin [\mu_s \pi z / (p+1)a] + C_s z / (p+1)a \} & \text{for } s=3,5, \dots, \end{cases} \tag{3}$$

where a is the width of a monolayer, pa is the well width, and μ_s and C_s are constants determined by $\tan(\mu_s \pi / 2) = \mu_s \pi / 2$ and $\Phi_s(z) = 0$ at $z = \pm(p+1)a/2$. A_s is a normalization constant. In our case, we are only interested in Raman scattering by the $s = 2$ LO-phonon mode. Keeping only the $s = 2$ term, we have

$$H_{e-ph}(z) = iA_2 \{ \cos [2\pi z / (d_1 + a)] + 1 \}, \tag{4}$$

where $d_1 = pa$ is the well width. We neglect the deformation-potential term in H_{e-ph} because it does not have any contribution in Raman scattering from the polarized A_1 mode.¹

We obtain exciton states using the \mathbf{k} -space sampling technique described in Ref. 2. Following the steps in Ref. 2, we first find the single-particle eigenstates for electron and hole in a superlattice, then expand the exciton

states in terms of linear combinations of the electron-hole product states. We briefly describe these procedures below. For an electron in the superlattice with wave vector $\mathbf{k} = (\mathbf{k}_\parallel, q)$, the wave function within the envelope-function approximation can be written as

$$\Phi_{n,\mathbf{k}}^e = \sum_{k_z} e^{i\mathbf{k}_\parallel \cdot \boldsymbol{\rho} + ik_z z} f_{n,q}(k_z) |u_C\rangle, \tag{5}$$

where $|u_C\rangle$ denotes the zone-center Bloch state of the well material and $k_z = s(2\pi/d)$, s =integer, d is the length of the superlattice. The zeroth-order m th valence-subband state at wave vector \mathbf{k} (or hole state at $-\mathbf{k}$) in the absence of the off-diagonal terms of the Luttinger Hamiltonian can be written as

$$\Phi_{m\nu,-\mathbf{k}}^{h0} = \sum_{k_z} e^{i\mathbf{k}_\parallel \cdot \boldsymbol{\rho} + ik_z z} g_{m\nu,q}^{h0}(k_z) |u_\nu\rangle, \tag{6}$$

where $\{|u_\nu\rangle; \nu = \frac{3}{2}, \frac{1}{2}, -\frac{1}{2}, -\frac{3}{2}\}$ are four bulk Bloch states at the valence-band maximum for the well material. The electron-hole product basis states are defined as

$$|nm\nu; \mathbf{k}_i\rangle = \sum_{\mathbf{k} \in \Delta_i} \Phi_{n,\mathbf{k}}^e \Phi_{m,\nu,-\mathbf{k}}^{h0}, \quad (7)$$

where $\sum_{\mathbf{k} \in \Delta_i}$ denotes a summation over wave vectors \mathbf{k} which fall inside a small \mathbf{k} -space sampling volume denoted Δ_i . Since the superlattice has cylindrical symmetry in the axial approximation,⁴ each \mathbf{k} -space sampling volume is a ring with small but finite width and thickness. The purpose for summing over \mathbf{k} within each sampling volume is to avoid divergence caused by the electron-hole interaction.

Now we expand our exciton states as

$$\Phi_{\text{ex}}^n = \sum_{m,\nu} \sum_i G_{m,\nu}^n(\mathbf{k}_i) |nm\nu; \mathbf{k}_i\rangle. \quad (8)$$

We have assumed that exciton states derived from different conduction subbands are decoupled, but those derived from different valence subbands are coupled. Thus, we include the effects of valence-band mixing but not the conduction-band mixing. This is justified because the energy separations between conduction subbands are much larger than the exciton binding energies. The expansion coefficients satisfy the following effective-mass equation:

$$\begin{aligned} [E_n^e(\mathbf{k}) - E_{m,\nu}^0(\mathbf{k}) - E_n^{\text{ex}}] G_{m,\nu}^n(\mathbf{k}_i) \\ + \sum_{m',\nu',i'} \left(v_{m,m',\nu}^n(\mathbf{k}_i, \mathbf{k}_{i'}) \delta_{\nu,\nu'} \right. \\ \left. - \sum_{k_z} H_{\nu,\nu'}^{\text{off}}(\mathbf{k}_i, \mathbf{k}_{i'}) \right) G_{m',\nu'}^n(\mathbf{k}_{i'}) = 0, \quad (9) \end{aligned}$$

where $v_{m,m',\nu}^n(\mathbf{k}_i, \mathbf{k}_{i'})$ denote the matrix elements of the electron-hole interaction and $H_{\nu,\nu'}^{\text{off}}(\mathbf{k}_i, \mathbf{k}_{i'})$ are off-diagonal matrix elements of the Kohn-Luttinger Hamiltonian. We solve this eigenvalue problem by diagonalizing the Hamiltonian H set up in our basis. For the superlattices with large barrier width, the adjacent quantum wells decouple, so we actually obtain solutions for multi-

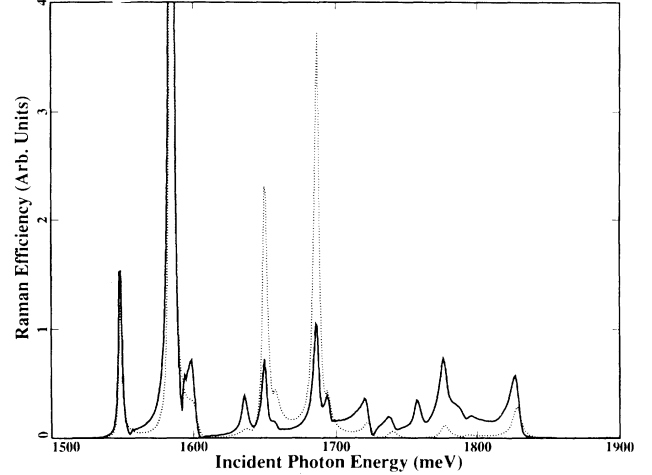


FIG. 1. Resonant Raman spectra for a 102-Å GaAs quantum well predicted from the present calculation. Solid curve: calculated spectrum with both discrete and continuum exciton states. Dotted curve: calculated spectrum with the omission of continuum exciton states.

ple quantum wells. In this case, only two sampling points for q are used.

The optical transition matrix element for heavy-hole (HH) excitons can be expressed as ($\alpha = \text{HH}n$)

$$\langle \alpha | P \cdot \hat{\epsilon} | 0 \rangle = \frac{1}{\sqrt{2}} \langle s | p_x | x \rangle \left(\sum_{m,k_i} G_{m,3/2}^{\text{HH}n}(\mathbf{k}_i) \langle f_n | g_m^{3/2} \rangle \right). \quad (10)$$

Similarly for light-hole (LH) excitons ($\alpha = \text{LH}n$),

$$\langle \alpha | P \cdot \hat{\epsilon} | 0 \rangle = \frac{1}{\sqrt{6}} \langle s | p_x | x \rangle \left(\sum_{m,k_i} G_{m,1/2}^{\text{LH}n}(\mathbf{k}_i) \langle f_n | g_m^{1/2} \rangle \right). \quad (11)$$

The Fröhlich interaction matrix element between two exciton states coupled to the A_1 LO mode is

$$\begin{aligned} \langle \beta | H_{e\text{-ph}} | \alpha \rangle = \sum_{m,\nu,k_i} G_{m,\nu}^n(\mathbf{k}_i) G_{m',\nu'}^{n'}(\mathbf{k}_i) \int f_n(z) f_{n'}^*(z) \left(1 + \cos \frac{2\pi z}{d_1 + a} \right) dz \\ - \delta_{n,n'} \sum_{m,m',\nu,k_i} G_{m,\nu}^n(\mathbf{k}_i) G_{m',\nu'}^{n'}(\mathbf{k}_i) \int g_{m\nu}(z) g_{m'\nu'}^*(z) \left(1 + \cos \frac{2\pi z}{d_1 + a} \right) dz. \quad (12) \end{aligned}$$

Selection rules are the same as those discussed in the paper by Zhu, Huang, and Tang.¹ In our calculation, we included the exciton states associated with the following subbands and symmetry types (given in parentheses): CB1-CB4(s), HH1-HH6(s), LH1-LH3(s, p). 300 \mathbf{k}_{\parallel} points are used in \mathbf{k} -space sampling for each pair of subbands. Note that the s -like HH exciton states are coupled with the p -like LH exciton states, whereas the s -like LH exciton states are coupled with the p -like HH exciton

states. The two sets of states led by s -like HH and s -like LH exciton states are not coupled. We find that the s -like LH set has about one-tenth the contribution of the s -like HH set, because the Raman strength is proportional to the square of the oscillator strength of excitons and the oscillator strength of the LH exciton is about one-third of the HH-exciton oscillator strength.² Thus the contributions due to s -like LH set can be ignored.

We have also included the nonparabolicity effect by

using energy-dependent effective masses given by

$$m_e^*(E_n^e) = m_e^*(0)/(1 + E_n^e/E_G)$$

and

$$m_v^*(E_m^v) = m_v^*(0)/(1 + E_m^v/E_G),$$

where E_G is the fundamental gap for bulk GaAs. The Luttinger parameters used in the present paper are taken from Ref. 5 for GaAs and from Ref. 6 for AlAs. Figure 1 shows the resonant-Raman-scattering (RRS) spectra of a 102-Å GaAs-Ga_{0.73}Al_{0.27}As quantum well. The spectra have been broadened by a Lorentzian function with half-width $\Gamma = 1.2, 2.0, 4.0,$ and 8.0 meV for CB1, CB2, CB3, and CB4 related transitions, respectively. The dotted curve is obtained by picking out those discrete exciton states while the solid curve is a final result which includes both the valence-band mixing and the effects of exciton continuum states. We found a dramatic difference between the two results both in magnitude and the line shape of the spectra. Without continuum states, the calculated Raman spectrum tends to be too high for photon energies between 1650 and 1700 meV and too low for photon energies above 1700 meV. The fact that adding contributions from the continuum states can reduce the Raman strength is interesting. This is a result of the cancellation effect, since contributions from different states can have different signs in the Raman tensor. The spectrum calculated by Zhu, Huang, and Tang¹ included the valence-band mixing but not the effects of continuum states. Their result is similar to the dotted curve shown in Fig. 1.

In Fig. 2 we compare our spectrum (lower half) with the experimental results taken from Ref. 2 (upper half). We also list the strengths of our top ten scattering channels in Table I. For comparison, the corresponding results from Ref. 1 are also included. Our values are consistently lower than those reported in Ref. 1. The difference may be due to differences in Luttinger parameters and in the basis functions used for the expansion of exciton states. The assignment of all prominent peaks in relation to their

TABLE I. Top ten scattering channels from our calculation for a 102-Å GaAs-Ga_{0.73}Al_{0.27}As quantum well (left) compared with the result taken from Ref. 1 (right).

Our result		Result from Ref. 1	
21L2p	-126.9	21L2p	-169.6
11H1s	-73.3	11H1s	-118.9
33H1s	-58.4	33H1s	-96.5
11H1s-31H1s	51.7		
11H1s-13H1s	32.3	11H1s-13H1s	138.6
22H1s	-27.2	22H1s	-90.4
21L2p-24H1s	23.9	21L2p-24H1s	39.8
31H1s-33H1s	-19.1		
13H1s-33H1s	-12.6	13H1s-33H1s	-37.9
21L2p-22H1s	-8.7	21L2p-22H1s	33.3
		22H1s-24H1s	64.8
		13H1s	39.8

energy positions is given in Table II. We have used the same notation as in Ref. 1 in which the first two numbers denote the principal quantum numbers of the electron and hole subbands; H or L denotes heavy hole or light hole; $1s$ or $2p$ denotes the ground state or first p -like excited exciton state; (in) or (out) denotes an incoming or outgoing resonance.

We find that all the prominent peaks observed in experiment match well with our prediction. A few more peaks predicted in our calculation [labeled 13H1s(out), 24H1s(in), 31H1s(in), and 24H1s(out)] are not obvious in the experimental observation, especially 13H1s(out) and 24H1s(in). For such well width, interband transition plays an important role. Our calculation also confirmed this point. The numerators for transitions to those two states are comparable to the numerators of other prominent transitions, as we can see from Table I, but in the measured spectrum we could hardly see anything nearby. We find that the Raman spectrum is somewhat sensitive to the broadening parameters due to the complicated interference effect. In the theoretical spectrum

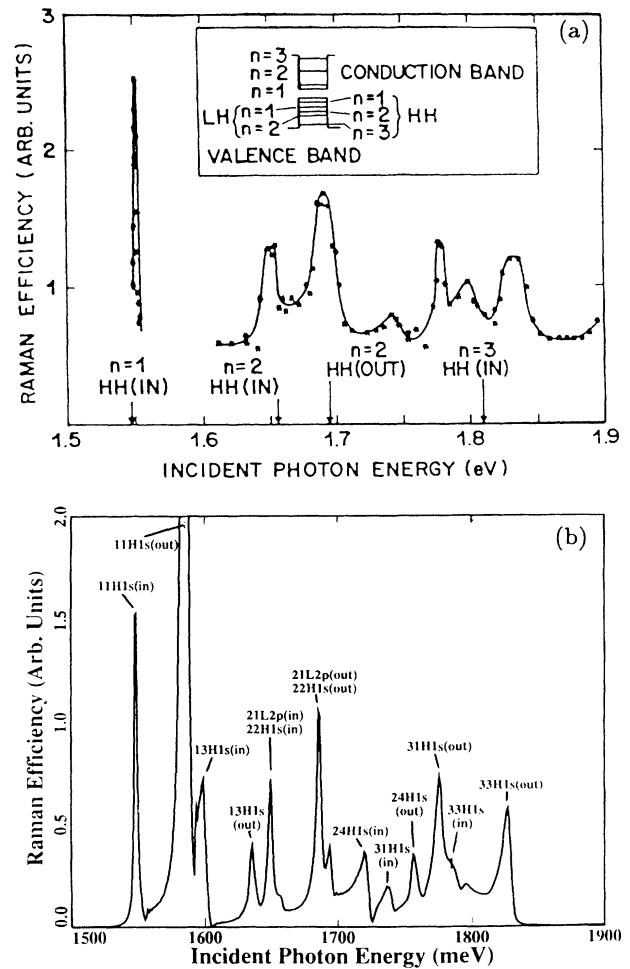


FIG. 2. Top: measured resonant Raman spectrum for a 102-Å GaAs quantum well (data taken from Ref. 3). Bottom: theoretical resonant Raman spectrum including both discrete and continuum exciton states.

TABLE II. Assignment of the prominent peaks in the resonant Raman spectrum of a 102-Å GaAs-Ga_{0.73}Al_{0.27}As quantum well.

Exciton state	$E(\text{meV})$ (theory)	Comment
11 $H1s$ (in)	1548.0	a
11 $H1s$ (out)	1585.3	b
13 $H1s$ (in)	1598.7	b
13 $H1s$ (out)	1637.3	c
22 $H1s$ (in) and 21 $L2p$ (in)	1650.7	a
22 $H1s$ (out) and 21 $L2p$ (out)	1686.7	a
24 $H1s$ (in)	1724.0	c
31 $H1s$ (in)	1738.7	a
24 $H1s$ (out)	1762.7	c
31 $H1s$ (out)	1776.0	a
33 $H1s$ (in)	1790	d
33 $H1s$ (out)	1826.7	a

^aPeak structure which is identified in the experiment and agrees with our calculation.

^bStrong luminescence effect, beyond the detectability of the experiment (Ref. 3).

^cPeak structures already present in the experimental spectrum, but not identified when a smooth interpolation curve was drawn in Ref. 3. Collecting more data can verify their existence.

^dA shoulder structure followed by a dip; seen in theoretical spectrum (not clearly seen in the measured spectrum); could be a Fano resonance.

shown in Fig. 2, we actually adopted a larger broadening parameter compared to other transitions involving the same conduction band in order to bring down the strengths of these two peaks. For example, we used $\Gamma=4.0$ meV for the 13 $H1s$ exciton and $\Gamma=3.0$ meV for the 24 $H1s$ exciton. We suspect that by collecting more data around those two exciton states, peak structures could be observed. There is one unidentified dip structure near $E = 1794$ meV which is seen in the theoretical spectrum. We suspect that this is a Fano-resonance structure caused by the interaction of the 33 $H1s$ exciton with the nearby continuum states. This feature is unclear in the measured spectrum due to an insufficient number of data points.

All of the incoming and outgoing resonant peaks are asymmetric as observed in experiment. It is the interference effect between intraband transition and interband transition that makes the incoming and outgoing resonance asymmetric. The strong coupling between the HH2-CB2 1s exciton and LH1-CB2 2p exciton is well known^{2,7} for this quantum well and it leads to a fine-structure splitting in the photoluminescence-excitation

spectrum.⁸ However, the fine-structure splitting is not resolved in the RRS spectrum. Our theoretical spectrum agrees well with data both in terms of peak positions and the relative intensities between incoming and outgoing resonant peaks. The agreement is significantly better than the previous calculation performed by Zhu, Huang, and Tang¹ which ignored the effects of exciton continuum states.

In summary, we have examined the effect of exciton continuum states on the RRS spectrum. We conclude that this effect cannot be neglected in determining the detailed line shape of the RRS spectrum. By including the effects of continuum states and nonparabolicity of higher bands, our predictions for peak positions and line shape of the RRS spectrum are in very good agreement with experiment.

This work was supported by the National Science Foundation (NSF) under Contract No. DMR-89-20538. The use of the National Center for Supercomputing Applications (NCSA) Cray Y-MP is acknowledged.

¹B. Zhu, K. Huang, and H. Tang, Phys. Rev. B **40**, 6299 (1989).

²Hanyou Chu and Y. C. Chang, Phys. Rev. B **39**, 10 861 (1989).

³E. Zucker, A. Pinczuk, D. S. Chemla, A. C. Gossard, and W. Wiegmann, Phys. Rev. Lett. **51**, 1293 (1983).

⁴M. Altarelli, Phys. Rev. B **32**, 5138 (1985).

⁵K. Hess, D. Bimberg, L. N. Lipari, T. V. Fischbach, and M.

Altarelli, in *Proceedings of 13th International Conference on the Physics of Semiconductors, Rome, 1976*, edited by F. G. Iurmi (North-Holland, Amsterdam, 1976), p. 142.

⁶P. Lawaetz, Phys. Rev. B **4**, 3460 (1971).

⁷B. Zhu and K. Huang, Phys. Rev. B **36**, 8102 (1987).

⁸R. Miller, A. C. Gossard, G. D. Sanders, Y. C. Chang, and J. N. Schulman, Phys. Rev. B **32**, 8452 (1985).